Reactions of $Os(CO)_4(\eta^2\text{-}C_2H_2)$ with Phosphines: Substitution and Facile CO Insertion into Osmium−Alkyne Bonds. Combined Synthetic and Kinetic Studies

Tienfu Mao, Zhongsheng Zhang, John Washington, J. Takats, and R. B. Jordan*

Department of Chemistry, University of Alberta, Edmonton, Alberta T6G 2G2, Canada

Received January 6, 1999

The reactions of $Os(CO)_4(\eta^2\text{-}C_2H_2)$ (**1**) with PMe_3 and P^tBu_3 are shown to yield an unexpectedly rich and diverse number of products. With excess PMe_3 at 0 °C, substitution of CO results in the mono(phosphine) (**2**) and bis(phosphine) (**3**) complexes as well as the CO-inserted osmacyclobutenone $Os(CO)_2(PMe_3)_2\{\eta^1{:}\eta^1\text{-}C(O)C_2H_2\}$ in two isomeric forms (**4a**,**b**). At ambient temperature, compound **3** transforms into the hydrido−acetylide species $Os(CO)_2(PMe_3)_2(H)(C_2H)$ (**7**), whereas **2** gives the bimetallic flyover bridged compound $Os_2(CO)_5(PMe_3)_2\{\mu\text{-}\eta^1{:}\eta^1{:}\eta^2\text{-}H_2C_2C(O)C_2H_2\}$ (**6**), identified on the basis of detailed multinuclear NMR spectroscopic studies. With excess P^tBu_3 at 0 °C, the only isolated product is the doubly CO inserted osmacyclopentene-2,4-dione $Os(CO)_3(P^tBu_3)(\eta^1{:}\eta^1\text{-}C(O)C_2H_2(O)C)$ (**5**), characterized further by X-ray crystallography. The rates of substitution of various phosphines on **1** to give the monophosphine complex are consistent with a dissociative mechanism, as found previously for the hexafluorobutyne analogue of **1**. For PMe_3, the rate constant and activation parameters are 3.0×10^{-2} s^{-1} (25 °C in pentane), $\Delta H_1^* = 90.7 \pm 1$ kJ mol^{-1}, and $\Delta S_1^* = 30.1 \pm 4$ J mol^{-1} K^{-1}. It is found that the η^2-C_2H_2 system is more reactive than the η^2-$C_2(CF_3)_2$ analogue, due to an ~9 kJ mol^{-1} lower ΔH_1^* value, as expected if the alkyne is acting as a four-electron donor to stabilize the dissociative intermediate. A detailed analysis of the P^tBu_3 system shows that the reaction proceeds through the monophosphine derivative, which reacts further with CO to give **5** and other products in amounts that depend on whether free CO is added to the system.

Introduction

Synthetic studies from this laboratory[1] have shown that $M(CO)_4(\eta^2\text{-alkyne})$ compounds (M = Fe, Ru, Os) have greatly enhanced reactivity compared to their $M(CO)_5$ parents. These compounds undergo fascinating reactions with $M(CO)_5$ (M = Ru, Os) and $(C_5R_5)M'(CO)_2$ (M′ = Co, Rh, Ir; R = H, Me) to give dimetallacyclic compounds,[1,2] and they undergo much more facile CO exchange and phosphine substitution reactions than the parents.[1] In a recent kinetic study,[3] we have shown that the replacement of CO by phosphines in the hexafluorobutyne complexes $M(CO)_4(\eta^2\text{-}C_2(CF_3)_2)$ is faster than in the $M(CO)_5$ parents by factors of 10^{13}, 10^3, and 10^6 for M = Fe, Ru, and Os, respectively. This remarkable increase in CO lability was attributed to the ability of the alkyne ligand to act as a 4-electron donor and thereby stabilize the formally 16-electron "$M(CO)_3L$" intermediate, as pictured in the following diagram:

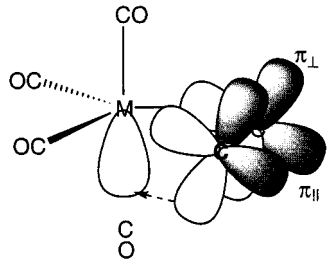

The present study was undertaken to test this hypothesis by studying the rate of CO substitution with a different alkyne. Specifically, the reactions of several phosphines with the acetylene complex $Os(CO)_4(\eta^2\text{-}C_2H_2)$ have been investigated. As a prelude to the kinetic study, synthetic work was carried out which revealed an unexpectedly rich variety of products, including facile and multiple CO insertions into the Os−acetylene bonds.

Results

Reactions of $Os(CO)_4(\eta^2\text{-}C_2H_2)$ with PR_3 (R = Me, ^{t}Bu). The reaction of $Os(CO)_4(\eta^2\text{-}C_2H_2)$ (**1**) with 1 equiv of PMe_3 proceeds readily and gives the monophosphine complex (**2**), as shown in eq 1. By NMR monitoring, it

(1) (a) Gagné, M. R.; Takats, J. *Organometallics* **1988**, *7*, 6850. (b) Burn, M. J.; Kiel, G.-Y.; Seils, F.; Takats, J.; Washington, J. *J. Am. Chem. Soc.* **1989**, *111*, 6850. (c) Takats, J. *J. Cluster Sci.* **1992**, *3*, 479. (d) Cooke, J.; Takats, J. *J. Am. Chem. Soc.* **1997**, *119*, 11088.

(2) Takats, J.; Washington, J.; Santarsiero, B. *Organometallics* **1994**, *13*, 1078.

(3) Pearson, J.; Cooke, J.; Takats, J.; Jordan, R. B. *J. Am. Chem. Soc.* **1998**, *120*, 1434.

10.1021/om990007t CCC: $18.00
Publication on Web 05/20/1999

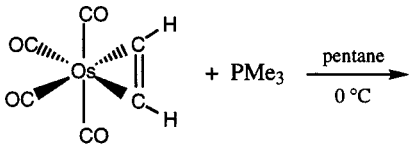

1

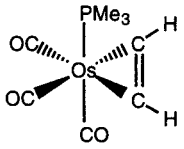

2 + CO (1)

was found that substitution of CO by PMe_3 starts around −30 °C and is synthetically convenient at 0 °C. After the solvent is stripped off at low temperature, the compound is isolated by sublimation as a thermally unstable yellow solid. The spectroscopic signatures are consistent with the structural formulation shown in eq 1. In particular, the ^{13}C NMR spectrum in the carbonyl region consists of two signals at 186.4 and 176.3 ppm in a 2:1 intensity ratio. The higher field carbonyl resonance exhibits a large $^{31}P-^{13}CO$ coupling ($^2J_{P-CO}$ = 116 Hz), as expected from the trans relationship of these two ligands as shown in **2**. Interestingly, and in contrast to the phosphine-substituted group VI $M(CO)_5PR_3$ (M = Cr, Mo, W) complexes,[4] the position of the CO ligand trans to PMe_3 is at higher field than the cis carbonyls. Full details of the synthetic procedures and spectroscopic properties of this and other complexes are given in the Experimental Section. The infrared bands of the various products are summarized in Table 1, as they are relevant to the kinetic studies described in a later section.

The reaction of $Os(CO)_4(\eta^2\text{-}C_2H_2)$ with a 10-fold excess of PMe_3 yielded three products. The spectroscopic features of these species allowed them to be identified as **3**, **4a**, and **4b**, with isolated yields of 32%, 26%, and 14%, respectively.

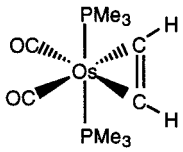

3

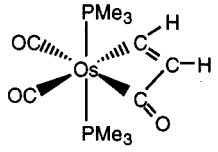

4a

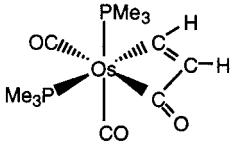

4b

The proposed composition of **3** is consistent with its mass spectrum and elemental analysis. The single resonance in the $^{31}P\{^1H\}$ NMR spectrum and, in particular, the virtual triplet of the CH_3 signal in the ^1H NMR spectrum show the trans arrangement of the PMe_3 ligands. This is consistent with the $^{13}C\{^1H\}$ NMR spectrum, which has one type of CO and one type of alkyne carbon. Compounds **4a** and **4b** have identical elemental analyses and very similar mass spectra. The single resonance in the $^{31}P\{^1H\}$ NMR spectrum of **4a** implies a trans arrangement of the PMe_3 ligands. The nonequivalent CO ligands are observed in the $^{13}C\{^1H\}$ NMR spectrum at δ 186.5 ($^2J_{CP}$ = 7.3 Hz) and δ 185.3 ($^2J_{CP}$ = 6.0 Hz). The $^{13}C\{^1H\}$ resonances of the $C_\beta HC_\alpha HC(O)$ moiety are as follows: δ 159.9 ($^2J_{C_\beta P}$ = 12.5 Hz), C_β; δ 166.7 ($^3J_{C_\alpha P}$ = 7.1 Hz), C_α; δ 213.4 ($^2J_{CP}$ = 10.8 Hz), C(O). The assignments are consistent with the established lower field position of the C_α carbon next to the acyl functionality and the expectation that $^2J_{C_\beta P} > {}^3J_{C_\alpha P}$. The $^{31}P\{^1H\}$ NMR spectrum of **4b** has two resonances at δ −44.4 and −50.1, indicating nonequivalent PMe_3 ligands. The CO ligands appear in the $^{13}C\{^1H\}$ NMR spectrum at δ 188.3 ($^2J_{CP}$ = 89.7 Hz, $^2J_{CP}$ = 7.7 Hz) and δ 186.5 ($^2J_{CP}$ = 9.7 Hz, $^2J_{CP}$ = 4.9 Hz). The large coupling ($^2J_{CP}$ = 89.7 Hz) indicates that the carbonyl at δ 188.3 is trans to one PMe_3. The ^{13}C chemical shifts of the $C_\beta HC_\alpha HC(O)$ group are similar to those of **4a**; the notable difference is that the C_β signal at δ 154.7 ($^2J_{C_\beta P}$ = 43.8 Hz, $^2J_{C_\beta P}$ = 13.3 Hz) has a large coupling to the ^{31}P at δ −50.1 (confirmed by selective ^{31}P decoupling). The magnitude of this coupling indicates that the β-carbon is trans to a PMe_3, consistent with the isomeric structure shown for **4b**.

Table 1. Important Infrared Bands for $Os(CO)_4(\eta^2\text{-}C_2H_2)$ + PR_3 Systems in Pentane

	ν, cm^{-1}	
compd	terminal CO str	acyl
$Os(CO)_4(\eta^2\text{-}C_2H_2)$ (**1**)	2122, 2035, 2026, 1994	
$Os(CO)_3(PMe_3)(\eta^2\text{-}C_2H_2)$ (**2**)	2056, 1977, 1947	
$Os(CO)_2(PMe_3)_2(\eta^2\text{-}C_2H_2)$ (**3**)	1998, 1897	
$Os(CO)_2(PMe_3)_2(OCC_2H_2)$ (**4a**)	1996, 1932	1652
$Os(CO)_2(PMe_3)_2(OCC_2H_2)$ (**4b**)	2010, 1938	1649
$Os(CO)_2(PMe_3)_2(H)(C_2H)$ (**7**)	2023, 1958	
$Os_2(CO)_5(PMe_3)_2\{C_2H_2C(O)C_2H_2\}$ (**6**)	2052, 2022, 1990, 1978, 1936	1605
$Os(CO)_3(P^tBu_3)(OCC_2H_2CO)$ (**5**)	2082, 2016, 1998	1614
$Os(CO)_3(PPh_3)(\eta^2\text{-}C_2H_2)$	2055, 1980, 1952	
$Os(CO)_3(P(OMe)_3)(\eta^2\text{-}C_2H_2)$	2059, 1977, 1947	

The reaction of **1** with 1 equiv of P^tBu_3 provided an unexpected, but interesting, contrast to that with PMe_3. Stirring the reaction mixture in pentane at 0 °C for 2−3 h resulted in the formation of a yellow precipitate of the doubly CO inserted product **5** in 42% yield. After the preliminary identification of this product, it was found that the yield could be increased to 61% if the reaction was done under an atmosphere of CO and in the presence of excess of P^tBu_3. The composition and spectroscopic properties of **5** are consistent with the structure shown, and this has been confirmed by X-ray crystallography (see next section). The $^{31}P\{^1H\}$ NMR spectrum of **5** has one resonance at δ −55.0. The $^{13}C\{^1H\}$ NMR shows two terminal carbonyls at δ 179.4 ($^2J_{CP}$ = 10.2 Hz) and δ 172.7 ($^2J_{CP}$ = 67 Hz) and the

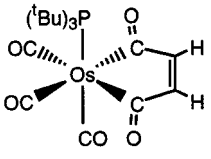

5

(4) Bodner, G. M. *Inorg. Chem.* **1975**, *14*, 2694. Bodner, G. M.; May, M. P.; McKinney, L. E. *Inorg. Chem.* **1980**, *19*, 1951.

acyl moieties at δ 246.6 ($^2J_{CP}$ = 7.9 Hz) with the expected intensity ratio of 2:1:2, respectively. In addition, the C_2H_2 group appears as a single resonance at δ 164.3. It is worth noting that similar doubly CO inserted products have been obtained from the analogous propyne and but-2-yne derivatives. Characterization of these complexes is detailed in the Experimental Section.

Another interesting difference is provided by the solution behavior of the mono- and bis-PMe_3 derivatives **2** and **3**, respectively. When a pentane solution of **2** is kept at room temperature for 12 h, an orange suspension is obtained. The elemental analysis and mass spectrum of this species indicate that it is a diosmium compound. On the basis of a detailed NMR study, including ^{13}CO-enriched material, selective ^{31}P decoupling, and ^{1}H−^{13}C shift-correlated 2D NMR experiments, structure **6** is assigned to this compound. For-

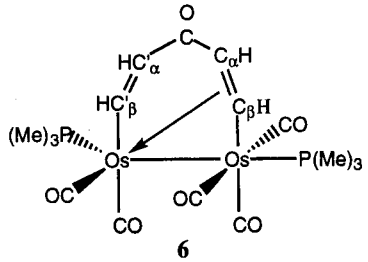

6

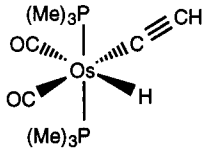

7

mation of dinuclear **6** is not unexpected, since we have observed previously[1b] facile addition of **1** to $M(CO)_5$ (M = Ru, Os), but the position of the inserted CO is somewhat unusual and will be discussed later. Although the bis(phosphine) derivative **3** also transforms into a new compound when kept in dichloromethane at ambient temperature for 2 h, the product is not dinuclear. The ^{1}H NMR spectrum of this species shows two triplets at δ −7.70 and 1.51 with an intensity ratio of 1:1; the PMe_3 protons resonate at δ 1.75. The high-field triplet is indicative of a hydride, while the signal at δ 1.51 is attributed to an acetylide hydrogen. The ^{13}C{^{1}H} NMR spectrum shows terminal carbonyls at δ 182.8 ($^2J_{CP}$ = 7.7 Hz) and δ 181.1 ($^2J_{CP}$ = 7.7 Hz) and carbons of the acetylide group at δ 93.4 ($^3J_{CP}$ = 2.7 Hz) and δ 87.0 ($^2J_{CP}$ = 17.2 Hz). The NMR data establish that the structure of **7** is as shown.

Molecular Structure of $Os(CO)_3(P^tBu_3)\{\eta^1:\eta^1\text{-}C(O)C_2H_2C(O)\}$ (5). The structure of **5** is shown in Figure 1, the crystal data and general conditions are given in Table 2, and selected bond distances and angles are given in Table 3. The X-ray study corroborates the spectroscopic deductions of the previous section. The osmium atom is bonded to three adjacent, terminal CO ligands, spanning one face of a distorted octahedron. The remaining three positions are occupied by the P^tBu_3 ligand and two C(O) groups inserted into the original Os−alkyne bonds, resulting in a "maleoyl" type of five-membered heterocyclic ring: an osmacyclopentenedione.

The distortions from octahedral geometry have their origin in the constraint imposed by the five-membered heterocyclic ring and the steric bulk of the P^tBu_3 ligand. The smaller than 90° C(4)−Os−C(7) angle (78.9(2)°) results in an opening of the opposite C(2)−Os−C(3) angle to 100.5(2)°; the remaining C−Os−C angles in this plane are near 90°. The large size of the P^tBu_3 ligand

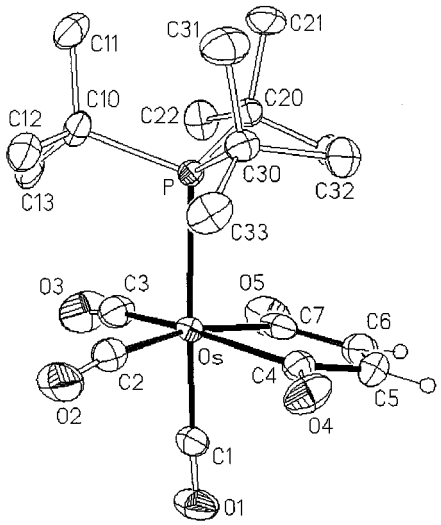

Figure 1. ORTEP view of $Os(CO)_3\{P^tBu_3\}\{\eta^2\text{-}C(O)C_2H_2C(O)\}$ (**5**). Probability ellipsoids are shown at the 50% level for non-hydrogen atoms.

Table 2. Summary of Crystallographic Data for 5

formula	$C_{19}H_{29}O_5OsP$
fw	558.59
cryst size (mm)	0.34 × 0.31 × 0.10
cryst syst	triclinic
space group	$P\bar{1}$ (No. 2)
a, Å	8.762(2)
b, Å	9.561(3)
c, Å	14.456(2)
α, deg	106.73(2)
β, deg	91.088(15)
γ, deg	114.25(2)
V, Å^3	1044.3(4)
Z	2
temp, °C	−50
D_{calcd}, g cm^{-3}	1.776
μ, mm^{-1}	6.207
radiation (λ, Å)	Mo Kα (0.710 73)
no. of rflns measd	7637 ($\pm h,k,l$)
no. of rflns used	3662 ($F_o^2 \geq -3\sigma(F_o^2)$)
no. of variables	235
R1 ($F_o^2 \geq 2\sigma(F_o^2)$)[a]	0.0253
wR2 (all data)[b]	0.0616

[a] $R1 = \Sigma||F_o| - |F_c||/\Sigma|F_o|$. [b] $wR2 = [\Sigma w(F_o^2 - F_c^2)^2/\Sigma w(F_o^4)]^{1/2}$.

manifests itself in the long Os−P bond distance. The observed value of 2.580(1) Å is ca. 0.2 Å longer than is typically found in organometallic osmium(II) compounds[5] and some 0.12 Å longer than the already long $Os-PMe^tBu_2$ distance (2.460(1) Å) in $OsCl\{C(CO_2Me)=CH_2\}(CO)(PMe^tBu_2)_2$.[6] The steric crowding results in a bending "down" of the osmacycle away from the phosphine ligand with P−Os−C(4) and P−Os−C(7) angles of 96.2(1) and 99.3(1)°, respectively. The C(3)O(3) carbonyl ligand also is slightly bent away from P^tBu_3 (P−Os−C(3) angle 93.3(1)°), and both equatorial carbonyl ligands deviate from linearity (Os−C(2)−O(2), 171.2(4)°; Os−C(3)−O(3), 168.4(2)°).

The Os−C(O) bond distances (2.137(4) and 2.134(4) Å) are similar to the Os−C(O)H length of 2.155(28) Å

(5) (a) Clark, G. R.; Headford, C. E. L.; Marsden, K.; Roper, W. R. *J. Organomet. Chem*. **1982**, *231*, 335. (b) Bellachioma, G.; Cardaci, G.; Machioni, A.; Zanazzi, P. *Inorg. Chem*. **1993**, *32*, 547. (c) Werner, H.; Knaup, W.; Shulz, M. *Chem. Ber*. **1991**, *124*, 1121. (d) Werner, H.; Esteruelas, M. A.; Otto, H. *Organometallics* **1986**, *5*, 2295.

(6) Werner, H.; Meyer, U.; Peters, K.; von Schnering, H. G. *Chem. Ber*. **1989**, *122*, 2097.

Table 3. Selected Bond Distances (Å) and Angles (deg) for 5

Os−C(1)	1.915(4)	Os−P	2.580(1)	C(1)−O(1)	1.121(5)
Os−C(2)	1.969(5)	C(4)−C(5)	1.506(6)	C(2)−O(2)	1.137(6)
Os−C(3)	1.956(5)	C(5)−C(6)	1.333(8)	C(3)−O(3)	1.135(6)
Os−C(4)	2.137(4)	C(6)−C(7)	1.482(7)	C(4)−O(4)	1.216(6)
Os−C(7)	2.134(4)			C(7)−O(5)	1.224(6)
P−Os−C(1)	178.1(1)	Os−C(1)−O(1)	176.8(4)	C(4)−Os−C(7)	78.9(2)
P−Os−C(2)	89.6(1)	Os−C(2)−O(2)	171.2(4)	C(4)−Os−C(2)	93.1(2)
P−Os−C(3)	93.3(1)	Os−C(3)−O(3)	168.2(4)	C(2)−Os−C(3)	100.5(2)
P−Os−C(4)	96.2(1)			C(3)−Os−C(7)	86.2(2)
P−Os−C(7)	99.3(1)				

in *trans*-[Os(CHO)(CO)(dppe)$_2$](SbF$_6$)[7] but perhaps slightly longer than other Os−C(sp^2) distances[5d,6,8] and imply little π-type interaction between these carbons and the metal. This is consistent with the lack of delocalization in the osmacyclopentenedione ring, and as expected, the C−O and C−C distances are similar to the corresponding values in related compounds containing ferracyclopentenedione rings, Fe(CO)$_4${η^1:η^1-C(O)C$_2$Et$_2$C(O)}[9a] and Fe(CO)$_4${η^1:η^1-C(O)C(CH$_3$)C(C$_2$-CH$_3$)(CO)}.[9b]

Reaction Kinetics. The major focus of this section is the kinetics of the first CO substitution in **1** by PR$_3$, as shown in eq 1. In some cases, subsequent reactions of **2** have been examined, as described by eq 2. The

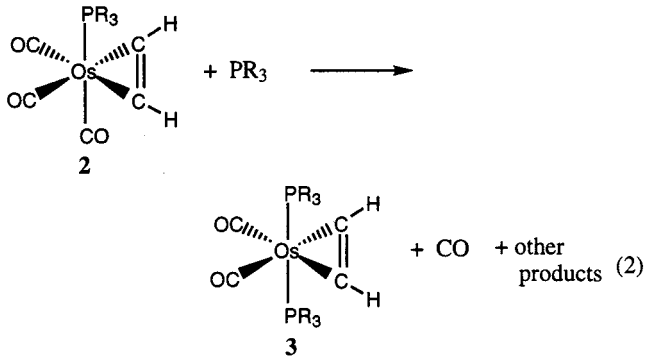

synthetic studies described above indicate that these reactions yield the disubstituted complex **3** and/or other products (depending on the nature of PR$_3$). Because of these chemical complications, the kinetic study has concentrated on reaction 1 by monitoring the rate of disappearance of Os(CO)$_4$(η^2-C$_2$H$_2$) at 2035 and 2026 cm^{-1}. For most of this work the solvent is pentane, because it provides the best resolution of the infrared bands. Studies have been done in dichloromethane to provide a direct comparison to the previous work on Os(CO)$_4$(η^2-C$_2$(CF$_3$)$_2$). Because PMe$_3$ is an important component of the synthetic studies, a typical time evolution of the infrared spectrum with this phosphine is shown in Figure 2. It is evident that the reaction cleanly produces **2**, although the final spectrum has very low intensity peaks at ~1930 and ~1895 cm^{-1} that may be assigned to **4a** and/or **4b** and to **3**, respectively.

The kinetic results are summarized in Tables 4−6. In all cases, the absorbance−time curves obey a first-order rate law. The data in Table 4 show that k_1, the rate constant for reaction 1, is independent of the concentration of PMe$_3$, and the observations in Table 5 show that k_1 is independent of the nature of the PR$_3$ entering group. The temperature dependence of k_1 (Table 4) is fitted well by the transition state theory equation to give $\Delta H_1^* = 90.7 \pm 1$ kJ mol^{-1} and $\Delta S_1^* = 30.1 \pm 4$ J mol^{-1} K^{-1} and a calculated value of $k_1 = 3.0 \times 10^{-2}$ s^{-1} at 25 °C.

The results for k_1 in dichloromethane are given in Table 6. The general kinetic behavior is the same as in pentane, and the rate constants are just slightly differ-

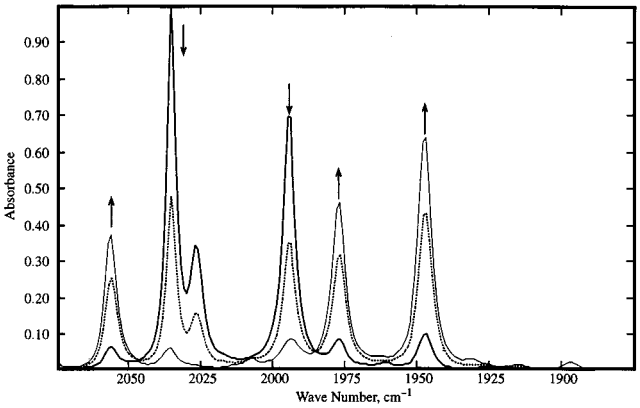

Figure 2. Representative infrared spectra for the reaction of 1.7 × 10^{-3} M Os(CO)$_4$(η^2-C$_2$H$_2$) with 0.077 M PMe$_3$ in pentane at 0 °C. The spectra shown were recorded at the following times (min) after mixing: 4.5 (—); 13.8 (···); 72.5 (—).

Table 4. Kinetic Results for the Reaction of Os(CO)$_4$(η^2-C$_2$H$_2$) with PMe$_3$ in Pentane

			$10^4 k_1$,[a] s^{-1}	
t, °C	10^3[Os(CO)$_4$(C$_2$H$_2$)], M	10^2[PMe$_3$], M	obsd	calcd[b]
−18.0	1.81	7.73	0.539	0.540
−13.1	1.81	7.73	1.14	1.23
−12.0	1.81	7.73	1.56	1.48
−5.0	1.81	2.90	4.57	4.51
−5.0	1.81	3.86	4.79	4.51
−5.0	1.81	7.73	4.62	4.51
−5.0	1.81	13.5	4.46	4.51
−5.0	1.81	19.3	4.65	4.51
−0.2	1.81	7.73	9.49	9.38
−0.1	1.23	0.615	9.19	9.52
0.0	0.938	0.656	9.73	9.66
0.0	1.23	0.615	9.36	9.66
0.0	1.23	0.615	9.36	9.66
0.0	1.81	7.73	9.76	9.66

[a] Determined from the decrease in absorbance of Os(CO)$_4$(η^2-C$_2$H$_2$) at 2035 cm^{-1}. [b] Calculated from least-squares fitting of the temperature dependence to the transition state theory equation with $\Delta H_1^* = 90.71$ kJ mol^{-1} and $\Delta S_1^* = 30.098$ J mol^{-1} K^{-1}. The standard deviations for ΔH_1^* and ΔS_1^* are ±1.1 kJ mol^{-1} and ±4.1 J mol^{-1} K^{-1}, respectively.

(7) Smith, G. S.; Cole-Hamilton, D. J.; Thornton-Pett, M.; Hursthouse, M. B. *J. Chem. Soc., Dalton Trans.* **1986**, 387.
(8) Espuelas, J.; Esteruelas, M. A.; Lahoz, F. J.; Oro, L. A.; Valero, C. *Organometallics* **1993**, *12*, 663.
(9) (a) Aime, S.; Milone, L.; Sappa, E.; Tiripicchio, A.; Manotti-Lanfredi, A. M. *J. Chem. Soc., Dalton Trans.* **1979**, 1664. (b) Pettersen, R. C.; Cihonski, J.; Young, F. R., III; Levenson, R. A. *J. Chem. Soc., Chem. Commun.* **1975**, 370.

Table 5. Kinetic Results for the Reaction of $Os(CO)_4(\eta^2\text{-}C_2H_2)$ with Various PR_3 Groups in Pentane at −5.0 °C

R_3	$[PR_3]$, M	E'_R,[a] kcal mol^{-1}	10^4k_1,[b] s^{-1}	k_2,[c] s^{-1}
Me_3	0.0290	26	4.57	8×10^{-6}
$(Me)_2Ph$	0.0181	33	4.42	1.4×10^{-4}
$Me(Ph)_2$	0.0181	39	4.51	6×10^{-5}
Ph_3	0.0181	43	4.62	1×10^{-4}
$(OMe)_3$	0.0181	48	4.96	1.5×10^{-4}
$(C_6H_{11})_3$	0.0181	67	4.64	1×10^{-3}
$^tBu_3$	0.0340	114	4.42	2×10^{-3} [d]

[a] Steric repulsion parameters as given by: Choi, M.-G.; Brown, T. L. *Inorg. Chem.* **1993**, *32*, 5603. [b] Determined from the decrease in absorbance of $Os(CO)_4(\eta^2\text{-}C_2H_2)$ at 2035 cm^{-1}; least-squares analysis gives a standard deviation of <2% on k_1. [c] Determined from the biphasic appearance and disappearance of $Os(CO)_3(PR_3)(\eta^2\text{-}C_2H_2)$ with k_1 fixed during the least-squares analysis, giving a standard deviation of <6% on k_2. [d] Determined from numerical integration as the value of k_1 in Scheme 3 and given in eq 8.

Table 6. Kinetic Results for the Reaction of $Os(CO)_4(\eta^2\text{-}C_2H_2)$ with PMe_3 and PPh_3 in Dichloromethane[a]

t, °C	phosphine	$10^2[PR_3]$, M	10^4k_1, s^{-1}
−17.9	PPh_3	4.42	0.617
−16.4	PMe_3	7.73	0.744
−11.4	PPh_3	4.42	2.00
−9.4	PMe_3	7.73	2.44
−5.0	PMe_3	7.73	4.47
−5.0	PPh_3	3.16	5.52
−5.0	PPh_3	4.42	5.60
−5.0	PPh_3	8.82	5.92
−0.6	PPh_3	4.42	10.0
−0.4	PPh_3	4.42	10.9
0.0	PMe_3	7.73	10.1
0.0	PMe_3	7.73	10.9

[a] All runs with 2.21×10^{-3} M $Os(CO)_4(\eta^2\text{-}C_2H_2)$, observed at 1939 and 1934 cm^{-1} for PMe_3 and PPh_3, respectively.

ent. The activation parameters for PMe_3 and PPh_3 are $\Delta H_1^* = 91.3 \pm 2$ and 92.0 ± 2 kJ mol^{-1} and $\Delta S_1^* = 33.0 \pm 9$ and 36.4 ± 8 J mol^{-1} K^{-1}, respectively. These parameters for the two phosphines agree well within their standard deviations and predict $k_1 \approx 3.2 \times 10^{-2}$ s^{-1} at 25 °C in dichloromethane. Clearly the solvent change from pentane to dichloromethane has a very minor effect on the kinetic parameters.

For reaction 2, the values of k_2 in Table 5 were determined at wavenumbers where the reaction shows biphasic behavior due to the formation and disappearance of **2**, so that k_2 refers to the net rate of disappearance of **2** to unspecified products. The second stage of the reaction was not followed to completion; therefore, k_2 is less well defined than k_1. The values of k_2 do depend on the nature of the spectator PR_3 ligand on **2** and very qualitatively increase with increasing value of the steric repulsion parameter E'_R. A correlation with the latter parameter was noted in the earlier study of the corresponding reaction of $Os(CO)_3(PR_3)(\eta^2\text{-}C_2(CF_3)_2)$ systems.[3]

The second stage of the reaction with P^tBu_3 does not correspond to formation of **3** but rather to **5** as the isolated product. The infrared spectra clearly show that **5** also is the major product under the conditions of the kinetic observations. This presents something of a problem, because **5** contains one more CO than the reactant **1**. Therefore, some other product(s) must be forming to provide the CO required by **5**. For example, the overall stoichiometry of the reaction might be

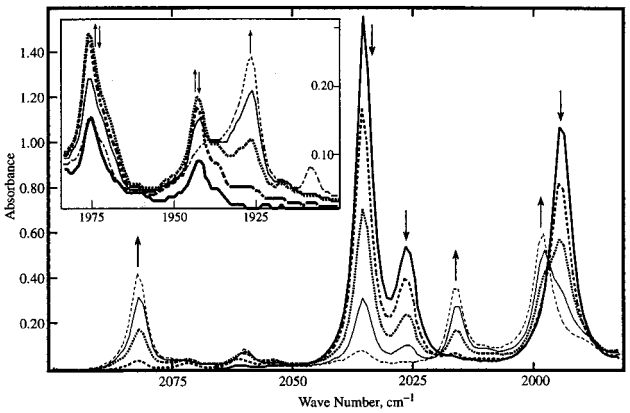

Figure 3. Representative infrared spectra for the reaction of 2.93×10^{-3} M $Os(CO)_4(\eta^2\text{-}C_2H_2)$ with 0.030 M P^tBu_3 in pentane at −5 °C. The inset shows the spectra on an expanded absorbance scale for the wavenumber region to the right of the main figure. Arrows indicate the direction of absorbance change with increasing reaction time. The spectra shown were recorded at the following times (min) after mixing: 4.6 (—); 17.5 (---); 36.8 (···); 69.0 (—); 141 (---).

represented by eq 3, 4, or 5, or some combination of

$$2Os(CO)_4(\eta^2\text{-}C_2H_2) + 2P^tBu_3 \rightarrow Os(CO)_3(P^tBu_3)(OCC_2H_2CO) + Os(CO)_3(P^tBu_3)(\eta^2\text{-}C_2H_2) \quad (3)$$

$$2Os(CO)_4(\eta^2\text{-}C_2H_2) + 3P^tBu_3 \rightarrow Os(CO)_3(P^tBu_3)(OCC_2H_2CO) + Os(CO)_2(P^tBu_3)_2(OCC_2H_2) \quad (4)$$

$$3Os(CO)_4(\eta^2\text{-}C_2H_2) + 4P^tBu_3 \rightarrow 2Os(CO)_3(P^tBu_3)(OCC_2H_2CO) + Os(CO)_2(P^tBu_3)(\eta^2\text{-}C_2H_2) \quad (5)$$

these. The other products in eqs 4 and 5 are suggested by the synthetic observations on the PMe_3 system. As a result, it is not surprising that other significant features appear in the spectra during the reaction.

Representative spectra from a kinetic run with P^tBu_3 in pentane are shown in Figure 3. The product (**5**) is observed to form at 2082 cm^{-1}, and the reactant (**1**) is detected at 2035 and 2026 cm^{-1}. An analysis of the absorbance−time curves for these species serves to characterize the major features of the reaction. The analysis has been done using numerical integration methods because the conditions, as given in Table 7, are not always pseudo-first-order. The analysis has been constrained by using the independently determined extinction coefficients of the reactant (**1**) and major product (**5**) and by making use of the fact that the extinction coefficients of observable intermediates and other products must have values that are independent of the reaction conditions. Representative results are shown in Figure 4. It was easily determined that the amount of **5** formed was essentially quantitative for run A, in which free CO was added, but essentially half of this amount is formed if the only source of CO is the reactant. This can be seen qualitatively from Figure 4, where the three runs have very similar total Os concentrations. This is consistent with the overall stoichiometry given by eq 3.

The analysis also revealed that the disappearance of **1** is independent of the P^tBu_3 concentration but is

Table 7. Reaction Conditions and Extinction Coefficients from Numerical Analysis for Kinetic Runs of the Reaction of $Os(CO)_4(\eta^2\text{-}C_2H_2)$ with P^tBu_3 at −5 °C in Pentane

	run				
	A	B	C	D	E
$[Os(CO)_4(C_2H_2)]$[a], mM	2.98	2.85	2.93	1.85	1.50
$[P^tBu_3]$,[a] mM	3.25	3.10	30.0	34.0	85.0
[CO],[a] mM	7.0				
$10^{-3}\epsilon$(2035),[b,c] **1**	10.6	10.8	10.8	11.3	11.1
$10^{-3}\epsilon$(2026),[b,c] **1**	4.2	4.2	4.4		
$10^{-3}\epsilon$(1977),[b,d] **2**	8.6	7.9	7.5	8.6	8.5
$10^{-3}\epsilon$(1944),[b,d] **2**	5.7	4.8	4.8	4.8	
$10^{-3}\epsilon$(2082),[b,c] **5**	6.0	5.8	5.7	5.7	5.8
$10^{-3}\epsilon$(2016),[b,c] **5**	4.9	4.8	4.8	4.9	4.8
$10^{-3}\epsilon$(1927),[b] **dimer**	8.0	8.2	8.0	8.0	7.5

[a] Initial concentration of reactant. [b] Extinction coefficient (M^{-1} cm^{-1}) at the wavenumber in parentheses for the species in bold type. [c] The independently determined values at the wavenumber in parentheses are as follows: 11.2×10^3 (2035), 4.3×10^3 (2026), 6.0×10^3 (2082), 5.1×10^3 (2016). [d] The dimer was assigned extinction coefficients of 3.2×10^3 (1977) and 2.2×10^3 (1944).

considerably slower when free CO is added, as also can be seen in Figure 4. This behavior is consistent with the usual dissociative mechanism shown in Scheme 1. This mechanism gives the rate law in eq 6, where the

$$-\frac{d[\mathbf{1}]}{dt} = \frac{k_d[\mathbf{1}]}{1 + \dfrac{k_c[CO]}{k_p[P^tBu_3]}} = \frac{4.5 \times 10^{-4}[\mathbf{1}]}{1 + 0.32\dfrac{[CO]}{[P^tBu_3]}} \qquad (6)$$

numerical values at −5 °C also are given. The k_d value is consistent with that of PMe_3 at −5 °C, given in Table 4. The term containing the competition ratio k_c/k_p is only significant for the runs with added CO or low P^tBu_3 concentration (runs A and B in Table 7).

The kinetics of the formation of **5** appear to follow the type of rate law expected for an "insertion" reaction in which the rate-controlling step is migration of an alkyne carbon in **2** to a coordinated CO. Then the unsaturated intermediate reacts with CO and the process is repeated in non-rate-controlling steps to give the final diacyl product, as shown in Scheme 2. If a steady state is assumed for the unsaturated intermediate, then the rate of formation of **5** is given by eq 7, where the numerical

$$\frac{d[\mathbf{5}]}{dt} = \frac{k_{2in}\left(\dfrac{k_{2ad}}{k_{2d}}\right)[CO][\mathbf{2}]}{1 + \dfrac{k_{2ad}}{k_{2d}}[CO]} = \frac{0.7 \times [CO][\mathbf{2}]}{1 + 100[CO]} \qquad (7)$$

values were obtained from fitting the data from various runs at −5 °C. Representative fits are shown in Figure 4. It should be noted that the rate of formation of **5** is significantly controlled by the rate of formation of **2**, so that the kinetic parameters in eq 7 have a more minor effect on the fit and are not as well-defined as those in eq 6.

The above analysis gives a very good quantitative description of the rates of reactant consumption and product formation. However, there are several features of the observations that remain unexplained. The above

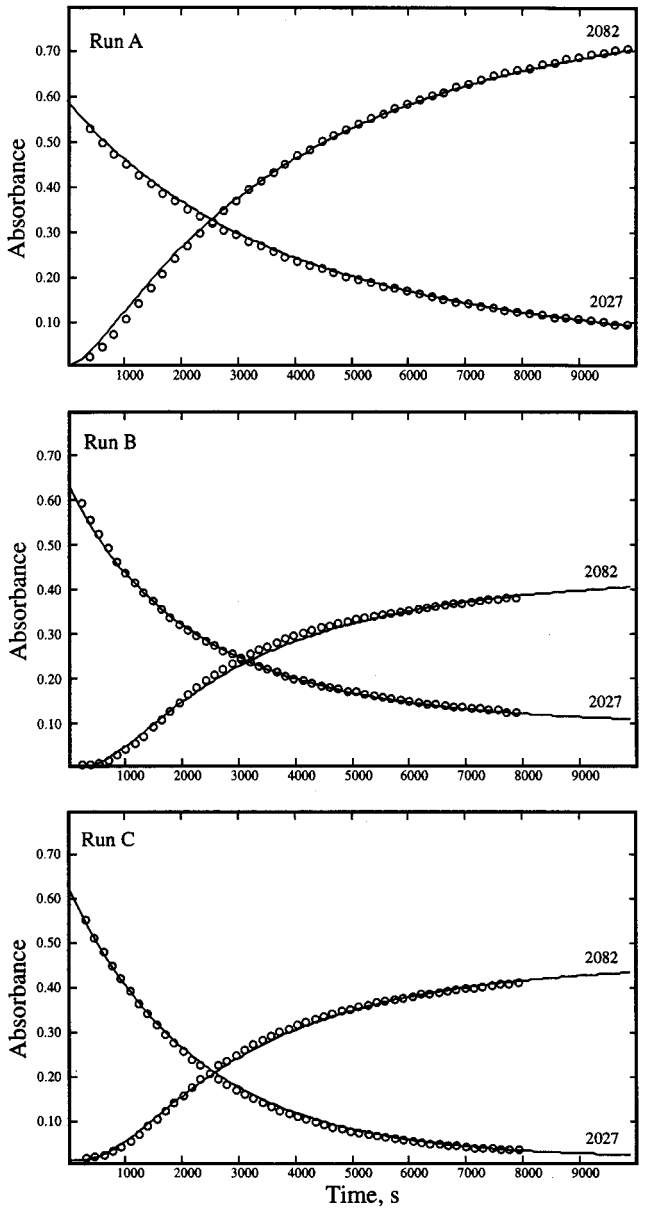

Figure 4. Representative time dependence of absorbance at the wavenumbers indicated for the reaction of $Os(CO)_4$-$(\eta^2\text{-}C_2H_2)$ with P^tBu_3 in pentane at −5 °C. The concentration conditions for runs A−C are given in Table 7.

Scheme 1

$$Os(CO)_4(C_2H_2) \underset{k_c}{\overset{k_d}{\rightleftharpoons}} \{Os(CO)_3(C_2H_2)\} + CO \xrightarrow[P^tBu_3]{k_P} Os(CO)_3(P^tBu_3)(C_2H_2)$$

1 **2**

model predicts that **2** should be produced and remain as 50% of the product, if no CO is added to the system. Therefore, one would expect to find bands in the infrared spectrum that would show the corresponding kinetic characteristics. In fact, two bands of significant intensity do appear at 1977 and 1944 cm^{-1} with a rate of growth that is consistent with formation of **2** from **1**. However, these bands show biphasic behavior, reaching a maximum after ∼1000 s and then slowly decreasing in intensity, as shown for the 1977 cm^{-1} band in Figure 5. By analogy to $Os(CO)_3(PMe_3)(\eta^2\text{-}C_2H_2)$, which has bands

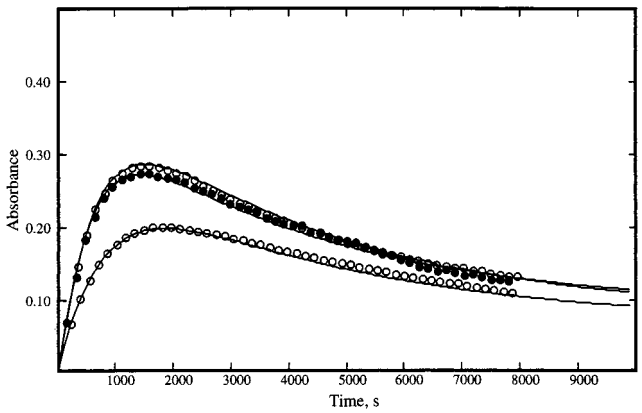

Figure 5. Absorbance changes at 1977 cm^{-1} for the reaction of $Os(CO)_4(\eta^2\text{-}C_2H_2)$ with P^tBu_3 in pentane at −5 °C. The data are for runs B (upper curve), C (●), and E (lower curve) with the concentrations given in Table 7.

Scheme 2

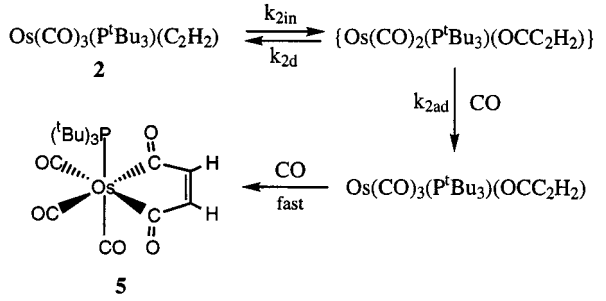

Scheme 3

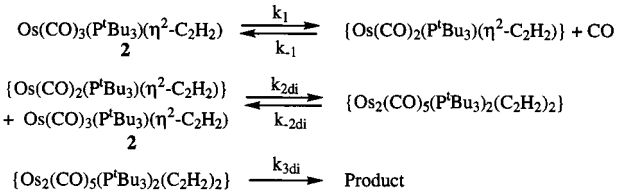

at 2056, 1977, and 1947 cm^{-1}, it seems reasonable to assign these bands to $Os(CO)_3(P^tBu_3)(\eta^2\text{-}C_2H_2)$ (**2**), but the model described above does not account for their decrease in intensity at long times. It appears that **2** is undergoing some transformation that is not associated with the formation of **5**; this conceivably could be an isomerization or a condensation reaction, on the basis of synthetic observations with PMe_3. A qualitative inspection reveals that the rate of this change appears to be independent of the phosphine and CO concentrations but seems to be slower at lower total Os concentrations. This is illustrated by the runs displayed in Figure 5, where the almost superimposable runs are at different phosphine concentrations while the third run is at a lower total Os concentration. This suggests a condensation to form a diosmium species, possibly analogous to **6** or its precursors. Kinetic studies[10] on condensation reactions of $Os(CO)_4(\eta^2\text{-}C_2H_2)$ with $Os(CO)_5$ and $Ru(CO)_5$ indicate that they proceed by rate-limiting dissociation of CO from $Os(CO)_4(\eta^2\text{-}C_2H_2)$, so that an analogous mechanism would seem probable for the present system. Therefore, the reaction sequence in

(10) Zhang, Z., Takats, J.; Jordan, R. B. To be submitted for publication,

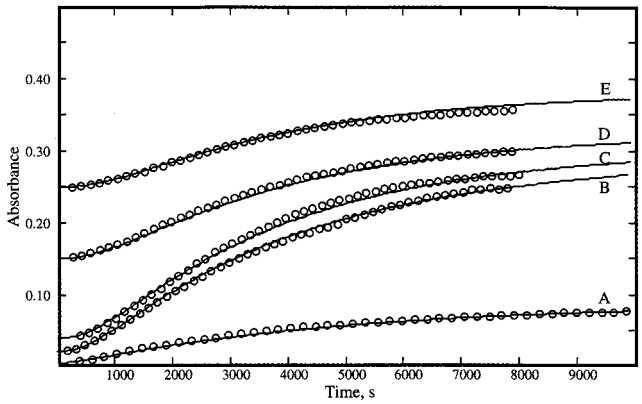

Figure 6. Absorbance changes at 1927 cm^{-1} for the reaction of $Os(CO)_4(\eta^2\text{-}C_2H_2)$ with P^tBu_3 in pentane at −5 °C. The letters correspond to the runs indicated in Table 7; curves B−E are displaced vertically from the initial zero absorbance for clarity of presentation.

Scheme 3 is suggested. If a steady state is assumed for the species in braces, then the rate of disappearance of **2** by this process is given by eq 8. This rate law will

$$-\frac{d[\mathbf{2}]}{dt} = \frac{2 \times k_1[\mathbf{2}]^2}{\frac{k_{-2di} + k_{3di}}{k_{2di}k_{3di}}k_{-1}[CO] + [\mathbf{2}]} = \frac{5 \times 10^{-3}[\mathbf{2}]^2}{20[CO] + [\mathbf{2}]} \quad (8)$$

give the second-order dependence on [**2**] if the first term in the denominator is larger than [**2**]. The numerical values given in eq 8 provide a reasonable representation of the rate of loss of **2**, but it should be noted that the value of 20 in the denominator is quite uncertain, except that it must be ≥5, and it is really the ratio of the numerical factors in the numerator and denominator that are defined by the data.

The above suggestion for the side reaction of **2** requires a modification of the reactions for the production of **5**. This is because the first reaction in Scheme 3 also is producing CO and this can react with **2** to give more **5**. The only parameter changes required to fit the observations are adjustments of the extinction coefficients.

The remaining feature of the infrared spectra that must be discussed is the absorbance at 1927 cm^{-1}. This feature is illustrated in Figure 6. The absorbance at 1927 cm^{-1} increases with time at a rate that closely parallels that of the formation of **5**. In fact, the proportion of this absorbance to that of **5** at 2082 cm^{-1} is essentially constant for the runs with different P^tBu_3 concentrations, but when CO is added, the absorbance at 1927 cm^{-1} is ∼$^1/_6$ of the value expected from the other runs. This can be seen by comparison of runs A and B in Figure 6. Apparently, the formation of the species absorbing at 1927 cm^{-1} relative to the major product, **5**, is independent of the phosphine concentration but is suppressed by added CO. These observations eliminate the possibility that the unknown species is an isomer of **5**, or a diacylated, bis(phosphine) complex.

One model that was tested assumed that the absorbance at 1927 cm^{-1} is due to the monoacylated species (**8**) that is the precursor of **5**. If **8** and **5** are effectively in rapid equilibrium, as described by eq 9, then the

$$\underset{\mathbf{8}}{Os(CO)_3(P^tBu_3)(CH_2CH_2CO)} + CO \overset{K}{\rightleftharpoons} \underset{\mathbf{5}}{Os(CO)_3(P^tBu_3)(OCCH_2CH_2CO)} \quad (9)$$

added CO would drive this equilibrium essentially completely to **5**; otherwise, the low final CO concentration would leave some of species **8** in the final product mixture. Quantitative analysis reveals that this will account for the relative changes in the absorbance at 1927 cm^{-1} between all the runs if $K \approx 3 \times 10^3$ M^{-1}. The model predicts that if **5** is dissolved in pentane, it should convert to about 30% **8** after about 1 h. However, when a solution of **5** in pentane was sealed in an infrared cell, the infrared spectrum remained unchanged over a period of 48 h at ambient temperature. Furthermore, when a ^{13}CO-enriched sample of **5** in pentane was sealed in an NMR tube and held at 50−55 °C for 3 h, there was no change in the NMR spectrum. Therefore, the equilibrium model is not viable.

Finally, it was concluded that the kinetic similarity of the absorbance at 1927 cm^{-1} and the formation of **5** was somewhat accidental and that the observations can be adequately explained if this absorbance is assigned to the dimer product in Scheme 3. The rate of formation of this species, taken from the absorbance decrease at 1977 cm^{-1}, is quite satisfactorily consistent with the rate of absorbance increase at 1927 cm^{-1}. Assignment of this peak to a dimer is consistent with the analogous dimer **6,** which has a peak at 1936 cm^{-1}. The final analysis has assumed minor absorbance from this species at 1977 and 1944 cm^{-1}, also based on analogy to **6** (see Table 1).

All of the curves in Figures 4−6 are calculated on the basis of this overall model. The extinction coefficients used are summarized in Table 7, and the general constancy of these values is taken as one measure of the validity of the proposed reactions.

Discussion

The main objective of the present study was to test our proposal that the enhanced lability of CO ligands in $M(CO)_4(\eta^2$-alkyne) complexes is due to the ability of the alkyne ligand to stabilize the formally 16-electron $\{M(CO)_3(\eta^2$-alkyne)$\}$ intermediate by 4-electron donation. If this is the case, then the rate of CO substitution should follow a predictable order based on the nature of the alkyne ligand.

As in our previous kinetic study,[3] the kinetic results for phosphine substitution on $Os(CO)_4(\eta^2$-$C_2H_2)$ show that the mechanism is dissociative, since the rate constant is independent of the concentration and nature of the phosphine. The rate constant of 3.0×10^{-2} s^{-1} (25 °C in pentane) is $\sim 10^7$ times larger than that for $Os(CO)_5$ and shows the tremendous activating effect of the alkyne ligand, as observed previously for hexafluorobutyne (HFB).

A comparison of the $Os(CO)_4(\eta^2$-$C_2H_2)$ and $Os(CO)_4$-$(\eta^2$-HFB) systems reveals that the former is ~10 times more reactive at 25 °C and the increased reactivity is primarily due to a 9 kJ mol^{-1} more favorable ΔH^*. This difference is consistent with and further strengthens our proposal that the alkyne is acting as a 4-electron donor to stabilize the dissociative transition state. Simple electronegativity arguments would predict that C_2H_2 is a better electron donor than HFB.

The synthetic work has revealed that the reactions of phosphine derivatives of $Os(CO)_4(\eta^2$-$C_2H_2)$ can proceed by CO insertions into the Os−alkyne bond(s). The facility and the number of inserted CO ligands depends on the nature of the phosphine ligand. Thus, with PMe_3 ligands, formation of only the monoacyl compounds **4a**,**b** is observed, whereas with P^tBu_3 insertion of two CO ligands occurs. In hindsight, these complications are not that surprising. Indeed, there is a vast body of literature dealing with transition-metal-mediated coupling of alkynes with carbon monoxide.[11] Yet, the formation of compounds **4a**,**b** and **5** from **1** represent some of the cleanest and most compelling examples for the initial steps of these coupling reactions at monometallic centers[12] en route to formation of cyclopentadienones and quinones. Although a number of maleoylmetal complexes related to **5** are known,[9,13] along with the methodology to convert some to the corresponding *p*-quinones,[14] we are aware of only two examples, both containing Ni,[15] where such compounds were formed by CO insertion into preexisting M−alkyne functionalities. The examples presented here underscore the dichotomy exhibited by osmium. The strength of the Os−C bond renders it uniquely suitable to allow isolation of models of the putative intermediates in metal-mediated organic transformations, yet the same strong bonds prevent further reactions.

There are several features of the reactivity patterns that deserve further comment. First of all, it is observed that the extent of CO insertion is greater with P^tBu_3 than with PMe_3. Since the σ-donor properties of these two phosphines are not greatly different, steric effects would seem to be the operative factor. This is consistent with the observations of Jablonski and Wang[16] on the methyl migration in *cis,cis*-$[(diars)Fe(CO)_2L(Me)]^+$, where L is various phosphines, whose cone angles correlate well with the reaction rates.

A more unexpected feature is that, under the conditions of the kinetic study, neither the tetracarbonyl−alkyne species (**1**) nor the *trans*-bis(phosphine)−dicarbonyl−alkyne species (**3**) undergoes CO insertion, but the monophosphine complexes are activated to CO insertion into the Os−alkyne bond. A rationalization of these observations requires some consideration as to

(11) (a) Hübel, W. In *Organic Synthesis via Metal Carbonyls*; Wender, I., Pino, P., Eds.; Wiley-Interscience: New York, 1968; Vol. 1, pp 273−340. (b) Pino, P.; Braca, G. In *Organic Synthesis via Metal Carbonyls*; Wender, I., Pino, P., Eds.; Wiley-Interscience: New York, 1977; Vol. 2, pp 420−516. (c) Davidson, J. L. In *Reactions of Coordinated Ligands*: Braterman, P. S., Ed.; Plenum Press: 1986: Vol. 1, pp 825−895. (d) Schore, N. E. *Chem. Rev.* **1988**, *88*, 1081. (e) Pearson, A. J.; Perosa, A. *Organometallics* **1995**, *14*, 5178. (f) Knölker, H.-J.; Baum, E.; Heber, J. *Tetrahedron Lett.* **1995**, *36*, 7647.

(12) For coupling of alkynes and CO on dimetallic centers see: (a) Mirza, H. A.; Vittal, J. J.; Puddephatt, R. J. *Organometallics* **1994**, *13*, 3063. (b) Hogarth, G.; Knox, S. A. R.; Lloyd, B. R.; Morton, D. A. V.; Orpen, A. J.; Turner, M. L. *Polyhedron* **1995**, *14*, 2723.

(13) (a) McVey, S.; Maitlis, P. M. *J. Organomet. Chem.* **1969**, *19*, 169. (b) Grevels, F.-W.; Buchremer, J.; Koerner von Gustorf, E. A. *J. Organomet. Chem.* **1976**, *111*, 225. (c) Corrigan, P. A., Dickson, R. S. *Aust. J. Chem.* **1979**, *32*, 2147.

(14) Liebeskind, L. S.; Baysdon, S. L.; South, M. S.; Iyer, S.; Leeds, J. P. *Tetrahedron* **1985**, *41*, 5839.

(15) (a) Hoberg, H.; Herrera, A. *Angew. Chem., Int. Ed. Engl.* **1980**, *19*, 927. (b) Bennett, M. A.; Hockless, D. C. R.; Humphrey, M. G.; Shultz, M.; Wenger, E. *Organometallics* **1996**, *15*, 928.

(16) Jablonski, C. R.; Wang, Y.-P. *Organometallics* **1990**, *9*, 318.

Scheme 4

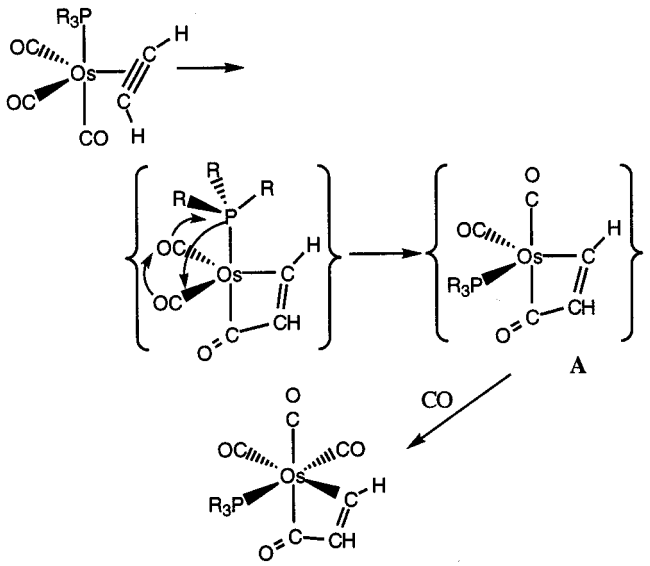

which CO ligand is involved in the migration process in the mono(phosphine) complexes. The geometry of the products seems to indicate that an equatorial CO is involved. However, the carbon of this CO is about 0.5 Å further from the alkyne C's than the axial CO.[17] This also provides an immediate rationalization for the fact that the *trans*-bis(phosphine) complex, which lacks an axial CO, does not undergo insertion. The problem is to explain how migration to an axial CO can result in the geometry of the observed products. A rationalization is offered by the sequence shown in Scheme 4. This suggests that the initially formed unsaturated intermediate undergoes a turnstyle-type rearrangement, driven by the steric interaction between the CH proton and the phosphine substituents so that a new trigonal bipyramid (**A**) is formed with the phosphine in an equatorial position. Because of the small bite angle of the acyl−alkene ligand, it is proposed that it prefers to span equatorial−axial positions rather than be in the equatorial plane. Addition of CO proceeds along the least sterically congested trigonal edge of the intermediate to give the monoacylated species. The formation of the monoacylated, bis(phosphine) species could occur by competition between PMe_3 and CO at this stage, and the absence of the analogous product with P^tBu_3 could be rationalized by steric effects, making the latter phosphine a less effective nucleophile than PMe_3. It should be noted that this mechanism predicts formation of the bis-PMe_3 complex with trans geometry (**4a**) but not that of the cis isomer (**4b**). The latter is the minor product, but simple bonding considerations would lead one to expect that it should be the more stable isomer because of better back-bonding to the CO trans to a PMe_3 ligand. Therefore, it is quite possible that **4b** is formed from **4a** by rearrangement and that the products isolated are under kinetic control.

Subsequent formation of the diacyl product can be rationalized on a similar basis, as shown in Scheme 5. The initial step would be migration to the CO trans to the phosphine of the product in Scheme 4 to produce

Scheme 5

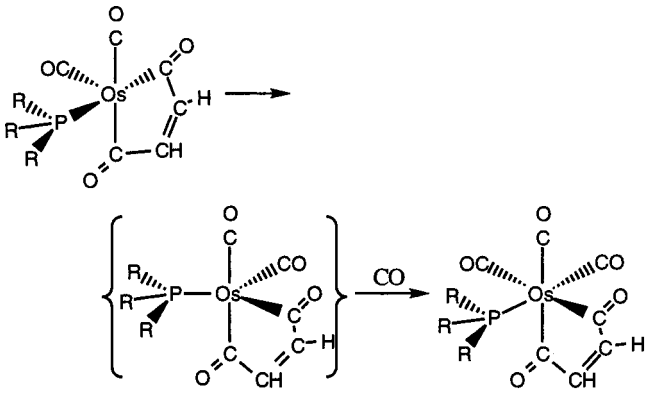

Scheme 6

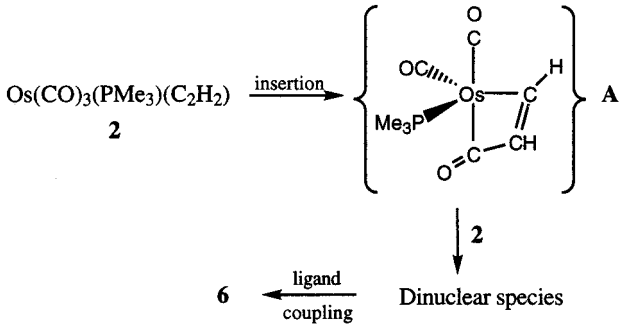

the first species shown in Scheme 5. The rearrangement could be driven by the interaction between the acyl oxygen and the phosphine substituents.

We reserve some final comments concerning the transformation of the monophosphine compound **2** to the dinuclear species **6**. In reality, this transformation is not that surprising. The CO ligands of **2** are labile, and we have amply demonstrated that such species are prone to further react with $M(CO)_5$ and $(C_5R_5)M'(CO)_2$ complexes to give bimetallic compounds.[1,10] However, this transformation, instead of yielding previously identified dimetallacyclobutene or dimetallacyclopentenone type products, gives a dimetallacycloheptadienone from the coupling of the two acetylene and one CO ligands. The compound is related to the well-known "flyover" complexes $M_2(CO)_{6-n}L_n\{\mu\text{-}\eta^1\text{:}\eta^1\text{:}\eta^4\text{-}(C_2R_2)_2CO\}$ (M = Fe, Ru; L = PPh_3, n = 1, 2; R = CH_3, Ph, H).[18] The difference is that the diosmium compound **6** has an extra terminal CO ligand and, consequently, only one of the double bonds of the "flyover" bridge is coordinated to the dimetal framework. This outcome can be explained by invoking the stronger Os−CO bond which, in this case, in contrast to the Fe and Ru complexes, resists elimination and coordination of the second olefinic double bond of the bridge. To rationalize the formation of **6**, we return to the CO insertion potential of compound **2** (vide supra) and note that **6** is formed under synthetic conditions in which there is no free PMe_3 or CO in solution. Then the reaction might proceed as shown in Scheme 6. The unsaturated 16-electron intermediate (**A**) formed during the insertion reaction of **2** reacts with remaining **2** to give a dinuclear species,

(17) Marinelli, G.; Streib, W. E.; Huffman, J. C.; Caulton, K. G.; Gagné, M. R.; Takats, J. Dartiguenave, M.; Chardon, C.; Jackson, S. A.; Eisenstein, O. *Polyhedron* **1990**, *9*, 1867.

(18) (a) Piron, J.; Piret, P.; Meunier-Piret, J.; Van Meerssche, M. *Bull. Soc. Chim. Belg.* **1969**, *78*, 121. (b) Cotton, F. A.; Hunter, D. L.; Troup, J. M. *Inorg. Chem.* **1976**, *15*, 63. (c) Aime, S.; Gobetto, R.; Nicola, G.; Osella, D.; Milone, L.; Rosenberg, E. *Organometallics* **1986**, *5*, 1829.

either via a donor−acceptor Os(**2**)→Os(**A**) bond or via donation from the $\pi_\perp$ orbital of the alkyne in **2**. This is followed by coupling between the acyl moiety and the alkyne ligand to produce **6**. The isolation of **6** opens the intriguing possibility that the mechanism of formation of dimetallacyclopentenones in reactions of $M(CO)_4(\eta^2$-alkyne) complexes with $M(CO)_5$ and $(C_5R_5)M'(CO)_2$ compounds may proceed, under certain conditions, via initial formation of a metallacyclobutenone followed by addition of the 18-electron reagent.

Experimental Section

General Procedures. All manipulations were performed under a static atmosphere of purified nitrogen or argon using standard Schlenk techniques. Solvents were dried by refluxing under nitrogen with the appropriate drying agent and were distilled just prior to use. CD_2Cl_2 was dried over P_2O_5 and vacuum-distilled, while $CDCl_3$ and toluene-d_8 were dried over molecular sieves prior to NMR sample preparation.

Infrared spectra were recorded on a Bomem MB-100 spectrometer with KBr windows having a 0.1 mm spacing. The ^{1}H, ^{31}P, and ^{13}C NMR spectra were recorded on Bruker AM-400, AM-300, and WH-200 spectrometers in CD_2Cl_2 unless otherwise indicated. The ^{1}H and ^{13}C chemical shifts (δ) were internally referenced to solvent and are reported in ppm relative to tetramethylsilane (TMS), while ^{31}P NMR chemical shifts were externally referenced to 85% H_3PO_4. The NMR sample tubes were flame-sealed under vacuum. Electron impact mass spectra were recorded on an AEI MS-12 spectrometer, operating at 70 eV. Elemental analyses were performed by the Microanalytical Laboratory of this department.

Preparation of $Os(CO)_3(PMe_3)(\eta^2\text{-}C_2H_2)$ (2). Trimethylphosphine (7.3 μL, 0.072 mmol) was added to a colorless solution of $Os(CO)_4(\eta^2\text{-}C_2H_2)$ (**1**; 23.5 mg, 0.072 mmol) in 15 mL of pentane at −78 °C. The solution was stirred and warmed slowly to ∼5 °C over a period of ca. 2 h. The solvent was removed in vacuo at −20 °C, and the residue was dried under vacuum. The compound is thermally unstable, and hence, elemental analysis is not available. For NMR characterization, the product was purified by sublimation in a closed system onto a dry ice cooled coldfinger, and the off-white solid was dissolved in CD_2Cl_2. Alternatively, material of purity suitable for further reactions or IR spectroscopy may be obtained by extracting the dried residue with pentane. Material enriched in ^{13}CO is obtained in the same way by starting with $Os(^{13}CO)_4(\eta^2\text{-}C_2H_2)$. IR (pentane, cm^{-1}): ν_{CO} 2056 s, 1977 s, 1947 s. ^{1}H NMR (−40 °C): 6.24 (d, J = 3.1 Hz, CH), 1.25 (d, J = 9.8 Hz, PMe_3). $^{13}C\{^1H\}$ NMR (−40 °C): 15.22 (d, J = 36.0 Hz, PMe_3), 83.13 (s, CH), 176.25 (d, J = 116 Hz, 1 CO), 186.42, (d, J = 11.0 Hz, 2 CO). $^{31}P\{^1H\}$ NMR (−40 °C): −46.05 (s).

Reaction of $Os(CO)_4(\eta^2\text{-}C_2H_2)$ with Excess PMe_3. Trimethylphosphine (3.1 mL, 29.9 mmol) was added to a colorless solution of $Os(CO)_4(\eta^2\text{-}C_2H_2)$ (**1**; 100 mg, 0.305 mmol) in 35 mL of pentane at 0 °C. The solution gradually turned yellow over 65 h at 0 °C. The yellow solution was then cooled to −78 °C, and the solvent was removed at this temperature to give a mixture of compounds: $Os(CO)_2(PMe_3)_2(\eta^2\text{-}C_2H_2)$ (**3**), *trans*-$Os(CO)_2(PMe_3)_2(\eta^2\text{-}C_2H_2C(O))$ (**4a**), and *cis*-$Os(CO)_2(PMe_3)_2(\eta^2\text{-}C_2H_2C(O))$ (**4b**). Sublimation in a closed vacuum system from −78 °C to ambient temperature gave 41 mg (32%) of **3** as a white solid. After sublimation the residue was separated by column chromatography employing silica gel and 70% THF/30% hexane as an eluting mixture. The first fraction proved to be **4b** (19 mg, 14%) as a yellow solid; the second fraction was **4a** (36 mg, 26%) as a yellow solid as well. The elemental analysis and spectroscopic data for these compounds are listed below.

3. Anal. Calcd for $C_{10}H_{20}O_2P_2Os$: C, 28.30; H, 4.75. Found: C, 28.58; H, 3.96. MS (FAB): $M^+ - nCO$, n = 0−2. IR (pentane, cm^{-1}): ν_{CO} 1998 m, 1897 s. ^{1}H NMR (−10 °C): 1.23 (t, J_{HP} = 3.7 Hz, 2PMe_3), 6.30 (t, $^3J_{HP}$ = 2.9 Hz, 2H). $^{31}P\{^1H\}$ NMR (−10 °C): −44.64 (s). $^{13}C\{^1H\}$ NMR (−20 °C): 192.5 (t, $^2J_{CP}$ = 8.9 Hz, CO), 94.5 (t, $^2J_{CP}$ = 2.6 Hz, C_2H_2), 16.9 (t, J_{CP} = 17.7 Hz, PMe_3).

4a. Anal. Calcd for $C_{11}H_{20}O_3P_2Os$: C, 29.20; H, 4.46. Found: C, 29.49; H, 4.41. MS (EI): $M^+ - nCO$, n = 0−2. IR (pentane, cm^{-1}): ν_{CO} 1996 m, 1932 s; ν_{acyl} 1652 w. ^{1}H NMR: 8.65 (dt, $^2J_{HH}$ = 6.9 Hz, $^3J_{PH}$ = 1.5 Hz, CH_β), 8.41 (dt, $^2J_{HH}$ = 6.9 Hz, $^3J_{PH}$ = 4.5 Hz, CH_α), 1.59 (virtual triplet, J_{PH} = 4.0 Hz, 2 PMe_3). $^{31}P\{^1H\}$ NMR: −41.49 (s). $^{13}C\{^1H\}$ NMR: 213.4 (t, $^2J_{CP}$ = 10.8 Hz, acyl), 186.5 (t, $^2J_{CP}$ = 7.3 Hz, 1 CO), 185.3 (t, $^2J_{CP}$ = 6.0 Hz, 1 CO), 166.7 (t, $^2J_{CP}$ = 7.1 Hz, Os−C(O)−C_αH), 155.9 (t, $^2J_{CP}$ = 12.5 Hz, Os−C_βH), 18.2 (t, $^1J_{CP}$ = 18.2 Hz, PMe_3).

4b. Anal. Calcd for $C_{11}H_{20}O_3P_2Os$: C, 29.20; H, 4.46. Found: C, 29.71; H, 3.98. IR (pentane, cm^{-1}): ν_{CO} 2010 s, 1938 vs; ν_{acyl} 1649 w. ^{1}H NMR: 8.83 (ddd, $^3J_{HH}$ = 6.2 Hz, $^3J_{P_aH}$ = 0.7 Hz, $^3J_{P_bH}$ = 3.1 Hz, H_β), 8.34 (ddd, $^3J_{HH}$ = 6.2 Hz, $^4J_{P_aH}$ = 4.2 Hz, $^4J_{P_bH}$ = 8.7 Hz, H_α), 1.68 (d, $^2J_{P_aH}$ = 9.2 Hz, P_bMe_3), 1.48 (d, $^2J_{P_bH}$ = 9.0 Hz, P_aMe_3). $^{31}P\{^1H\}$ NMR: P_a, −44.4 (d, $^2J_{PP}$ = 21 Hz); P_b, −50.1 (d, $^2J_{PP}$ = 21 Hz). $^{13}C\{^1H\}$ NMR (−10 °C): 207.8 (dd, $^2J_{CP}$ = 11.4 Hz, $^2J_{CP}$ = 3.7 Hz, acyl), 188.3 (dd, $^2J_{CP}$ = 89.7 Hz, $^2J_{CP}$ = 7.7 Hz, 1 CO), 186.5 (dd, $^2J_{CP}$ = 9.7 Hz, $^2J_{CP}$ = 4.9 Hz, 1 CO), 166.3 (d, $^3J_{CP}$ = 6.5 Hz, Os−C(O)−C_αH), 154.7 (dd, $^2J_{CP_b}$ = 43.8 Hz, $^2J_{CP_a}$ = 13.3 Hz, Os−C_βH), 20.0 (d, $^1J_{CP}$ = 32.6 Hz, PMe_3), 16.0 (d, $^1J_{CP}$ = 34.0 Hz, PMe_3).

Synthesis of $Os(CO)_3\{P^tBu_3\}\{\eta^1\text{:}\eta^1\text{-}C(O)C_2H_2C(O)\}$ (5). A precooled (−78 °C) flask was charged with 25 mL of pentane, $Os(CO)_4(\eta^2\text{-}C_2H_2)$ (52.5 mg, 0.16 mmol), and P^tBu_3 (300 mg, 1.49 mmol). The flask was subject to a freeze−pump−thaw cycle, after which ca. 1 atm of CO was admitted into the flask. The resulting colorless solution was slowly warmed to 10 °C to yield a light orange solution and an orange precipitate. The precipitate was isolated and washed with pentane (2 × 10 mL) to yield 54.5 mg (61%) of **5** as an orange solid. Anal. Calcd for $C_{19}H_{29}O_5OsP$: C: 40.85, H: 5.23. Found; C: 41.32, H: 5.11. IR (pentane, cm^{-1}): ν_{CO} 2081 s, 2016 m, 1998 s; ν_{acyl} 1614 w. ^{1}H NMR: 6.80 (d, $^4J_{PH}$ = 0.6 Hz, 2 H), 1.50 (d, $^3J_{PH}$ = 8.1 Hz, 27 H). $^{31}P\{^1H\}$ NMR: −57.1 (s). $^{13}C\{^1H\}$ NMR: 246.7 (d, $^2J_{CP}$ = 7.6 Hz, 2(acyl)), 179.5 (d, $^2J_{CP}$ = 9.7 Hz, 2 CO), 172.7 (d, $^2J_{CP}$ = 66.9 Hz, 1 CO), 164.3 (s, C_2H_2), 43.7 (d, $^2J_{CP}$ = 11.5 Hz, P(CMe_3)$_3$), 33.1 (br, P(CMe_3)$_3$).

Synthesis of $Os(CO)_3\{P^tBu_3\}\{\eta^1\text{:}\eta^1\text{-}C(O)CHCCH_3C(O)\}$. The procedure described above for **5** was used, starting with $Os(CO)_4(\eta^2\text{-}CHCCH_3)$ (11.2 mg, 0.033 mmol) and P^tBu_3 (150 mg, 0.74 mmol). The product was isolated and washed as above to yield 8.1 mg (45%) of an orange solid. Anal. Calcd for $C_{20}H_{31}O_5OsP$: C: 41.95, H: 5.46. Found; C: 41.50, H: 5.10. IR (pentane, cm^{-1}): ν_{CO} 2079 s, 2012 m, 1994 s; ν_{acyl} 1622 w. ^{1}H NMR: 6.85 (q, $^4J_{HH}$ = 1.0 Hz, 1 H), 1.88 (d, $^4J_{HH}$ = 1.0 Hz, 3 H), 1.5 (d, $^3J_{PH}$ = 8.2 Hz, 27 H). $^{31}P\{^1H\}$ NMR: −55.5 (s). $^{13}C\{^1H\}$ NMR: 244.9 (d, $^2J_{CP}$ = 7.4 Hz, 1(acyl)), 243.1 (d, $^2J_{CP}$ = 7.4 Hz, 1(acyl)), 179.7 (d, $^2J_{CP}$ = 10.2 Hz, 1 CO), 179.5 (d, $^2J_{CP}$ = 10.2 Hz, 1 CO), 173.0 (d, $^2J_{CP}$ = 67.3 Hz, 1 CO), 173.6 (s, CCH_3), 161.6 (s, CCH), 43.5 (d, $^2J_{CP}$ = 11.2 Hz, P(CMe_3)$_3$), 33.1 (br, P(CMe_3)$_3$), 11.9 (s, CCH_3).

Synthesis of $Os(CO)_3\{P^tBu_3\}\{\eta^1\text{:}\eta^1\text{-}C(O)C_2(CH_3)_2C(O)\}$. The procedure described above for **5** was used, starting with $Os(CO)_4(\eta^2\text{-}C_2(CH_3)_2)$ (21.0 mg, 0.059 mmol) and P^tBu_3 (400 mg, 1.98 mmol). The product was isolated and washed as above to yield 19.1 mg (58%) of an orange solid. Anal. Calcd for $C_{21}H_{33}O_5OsP$: C: 42.99, H: 5.67. Found; C: 42.93, H: 5.59. IR (pentane, cm^{-1}): ν_{CO} 2078 s, 2012 m, 1994 s; ν_{acyl} 1608 w. ^{1}H NMR: 1.77 (d, $^4J_{HH}$ = 1.0 Hz, 6 H), 1.42 (d, $^3J_{PH}$ = 8.2 Hz, 27 H). $^{31}P\{^1H\}$ NMR: −54.2 (s). $^{13}C\{^1H\}$ NMR: 242.9 (d, $^2J_{CP}$ = 7.8 Hz, 2(acyl)), 179.8 (d, $^2J_{CP}$ = 10.6 Hz, 2 CO), 173.7 (d, $^2J_{CP}$ = 68.8 Hz, 1 CO), 168.2 (s, CCH_3), 43.4 (d, $^2J_{CP}$ = 11.5 Hz, P(CMe_3)$_3$), 33.2 (br, P(CMe_3)$_3$), 10.8 (s, CCH_3).

Synthesis of $Os(CO)_2(PMe_3)_2(H)(C_2H)$ (7). A colorless solution of compound **3** (15 mg, 0.353 mmol) in 5 mL of CH_2Cl_2 was warmed to room temperature. After the mixture was stirred for 2 h, the solvent was stripped off in vacuo. Recrystallization from pentane gave **7** (9 mg, 60%) as a white powder. Anal. Calcd for $C_{10}H_{20}O_2P_2Os$: C, 28.30; H, 4.75. Found: C, 28.33; H, 4.55. IR (pentane, cm^{-1}): ν_{CO} 2023 m, 1958 s. ^1H NMR: −7.70 (t, $^2J_{PH}$ = 22.2 Hz, 1H), 1.51 (t, $^4J_{PH}$ = 4.1 Hz, C_2H), 1.75 (t, J_{PH} = 4.1 Hz, 2 PMe_3). $^{31}P\{^1H\}$ NMR: −47.0 (s). $^{13}C\{^1H\}$ NMR: 182.8 (t, $^2J_{CP}$ = 7.7 Hz, 1 CO), 181.1 (t, $^2J_{CP}$ = 7.7 Hz, 1CO), 93.4 (t, $^3J_{CP}$ = 2.7 Hz, *C*CH), 87.0 (t, $^2J_{CP}$ = 17.2 Hz, *C*CH), 21.0 (t, J_{CP} = 19.0 Hz, PMe_3).

Synthesis of $Os_2(CO)_5(PMe_3)_2\{\mu\text{-}\eta^1\text{:}\eta^2\text{-}C_2H_2C(O)C_2H_2\}$ (6). Trimethylphosphine (28.9 mL, 0.279 mmol) was added to a solution of $Os(CO)_4(\eta^2\text{-}C_2H_2)$ (91.7 mg, 0.279 mmol) in 35 mL of pentane at 0 °C. The colorless solution was stirred at 0 °C for 3 h; it gradually turned yellow. The yellow solution was warmed to room temperature, resulting in the formation of an orange precipitate. The mixture was stirred for an additional 12 h, and then the solvent was removed in vacuo. The residue was washed by adding 5 mL of hexane at room temperature and stirring for a few minutes, followed by cooling to −78 °C. The supernatant was then removed by syringe. After this process was repeated three times, the resulting yellow powder was dried under vacuum. The yield of **6** was 62 mg (59%). Anal. Calcd for $C_{16}H_{22}O_6P_2Os_2$: C, 25.53; H, 2.95. Found: C, 25.09; H, 2.74. MS (70 eV, 200 °C, *m/e*): $M^+ - n$CO, n = 0−5. IR (pentane, cm^{-1}): ν_{CO} 2052 m, 2022 m, 1990 vs, 1978 s, 1936 m; ν_{acyl} 1605 w. IR (pentane, cm^{-1}, with ^{13}CO-enriched product): ν_{CO} 2006 m, 1973 m, 1944 vs, 1934 s, 1904 m; ν_{acyl} 1570 w. ^1H NMR: H'_β, 9.30 (dd, $^3J_{H'_\alpha H'_\beta}$ = 12.6 Hz, $^2J_{P_\alpha H'_\beta}$ = 5.4 Hz); H_β, 8.79 (d, $^3J_{H_\alpha H_\beta}$ = 9.3 Hz), H'_α, 6.25 (ddd, $^3J_{H'_\alpha H'_\beta}$ = 12.6 Hz, $^4J_{P_a H'_\alpha}$= 2.2 Hz, $^3J_{H_\alpha H'_\alpha}$ = 1.0 Hz); H_α, 4.65 (ddd, $^3J_{H_\alpha H_\beta}$ = 9.3 Hz, $^3J_{P_b H_\alpha}$ = 6.0 Hz, $^3J_{H_\alpha H'_\alpha}$ = 1.0 Hz); H_{P_b}, 1.88 (d, $^2J_{P_b H}$ = 10.6 Hz, 9H); H_{P_a}, 1.83 (d, $^2J_{P_a H}$ = 10.7 Hz, 9H). $^{31}P\{^1H\}$ NMR: P_a, −31.2 (s); P_b, −51.1 (s). $^{13}C\{^1H\}$ NMR: 202.0 (s, acyl), 191.1 (dd, $^3J_{CP_a}$ = 4.8 Hz, $^2J_{CP_b}$ = 6.4 Hz, 1 $C_{c/d}O$), 189.5 (d, $^2J_{CP_a}$ = 6.4 Hz, l $C_{a/b}O$), 188.4 (d, $^2J_{CP_b}$ = 6.3 Hz, l $C_{c/d}O$), 183.8 (d, $^2J_{CP_a}$ = 6.3 Hz, 1 $C_{a/b}O$), 180.5 (s, 1 C_eO), 173.8 (d, $^2J_{CP_a}$ = 8.3 Hz, CH'_β), 134.9 (s, CH_β), 131.9 (s, CH'_α), 64.9 (c, CH_α), 22.6 (d, $^1J_{CP_a}$ = 39.6 Hz, P_aMe_3), 19.5 (d, $^1J_{CP_b}$ = 37.9 Hz, P_bMe_3). $^{13}C\{^1H\}$ NMR (with ^{13}CO-enriched product): 202.0 (s, acyl), 191.1 (ddd, $^3J_{CP_a}$ = 4.8 Hz, $^2J_{CP_b}$ = 6.4 Hz, $^2J_{CC}$ = 34.5 Hz, 1 $C_{c/d}O$), 189.5 (d, $^2J_{CP_a}$ = 6.4 Hz, 1 $C_{a/b}O$), 188.4 (dd, $^2J_{CP_b}$ = 6.3 Hz, $^2J_{CC}$ = 34.5 Hz, 1 $C_{c/d}O$), 183.8 (d, $^2J_{CP_a}$ = 6.3 Hz, 1 $C_{a/b}O$), 180.5 (s, 1 C_eO), 173.8 (dd, $^2J_{CPa}$ = 8.3 Hz, $^2J_{CC}$ 17.7 Hz, CH'_β), 134.9 (d, $^2J_{CC}$ = 21.5 Hz, CH_β), 131.9 (d, $^2J_{CC}$ = 55.8 Hz, $C_{H'_\alpha}$), 64.9 (d, $^2J_{CC}$ = 49.7 Hz, CH_α), 22.6 (d, $^1J_{CP_a}$ = 39.6 Hz, P_aMe_3), 19.5 (d, $^1J_{CP_b}$ = 37.9 Hz, P_bMe_3). ^{13}C NMR: 173.8 (dd, $^2J_{CP_a}$ = 8.3 Hz, $^1J_{CH}$ = 132 Hz, CH'_β), 134.9 (d, $^1J_{CH}$ = 141.7 Hz, CH_β), 131.9 (d, $^1J_{CH}$ = 155.3 Hz, CH'_α), 64.9 (d, $^1J_{CH}$ = 151.9 Hz, CH_α), 22.6 (dm, $^1J_{CP_a}$ = 39.6 Hz, P_aMe_3), 19.5 (dm, $^1J_{CP_b}$ = 37.9 Hz, P_bMe_3).

X-ray Crystal Structure Analysis of $Os(CO)_3(P^tBu_3)\{\eta^1\text{:}\eta^1\text{-}C(O)C_2H_2C(O)\}$ (5). An X-ray-quality crystal of **5**, grown by slow cooling of a CH_2Cl_2/hexane (1:5) solution of **5** to −5 °C, was mounted on the goniometer of an Enraf-Nonius CAD4 diffractometer. The structure was solved using the methods of SHELXS-86[19] and refined with SHELXS-93.[20] Reflection data were corrected for absorption using the method of Walker and Stuart.[21] The crystal data and general conditions of data collection and structure refinement are given in Table 2.

Kinetic Methods. For the solid phosphines, equal weighed amounts of phosphine were added to each of two 1.0 mL volumetric flasks sealed with serum caps and the flasks were purged with dry nitrogen. Then an appropriate volume of solvent was added by syringe to each flask and the flasks were placed in a dry ice−acetone bath. For liquid PMe_3, the PMe_3 was added from a syringe at this stage. A sample from one flask was transferred with a precooled syringe to the infrared cell, and the blank spectrum was recorded. An appropriate volume of a stock solution of $Os(CO)_4(\eta^2\text{-}C_2H_2)$ was added to the other flask, and a sample of this solution was transferred to the infrared cell as before. When CO was added, the solution containing all reactants at dry ice temperature was purged with CO for 10−15 min and then brought to within 5 °C of the reaction temperature before stopping the CO purge and transferring a sample to the infrared cell. The CO concentration was estimated from literature data.[22]

In all cases, the infrared cell was preequilibrated at the desired temperature for 30 min before use. Temperature was maintained to ±0.1 °C with a liquid circulating system described previously,[3] and the temperature of the cell was continuously monitored with a copper−constantan thermocouple. The infrared cell (Graseby Specac) was a gastight model with CaF_2 windows, amalgamated foil spacer and gaskets, and a stainless steel body. The path length of the cell was determined to be 0.0475 cm.

The operation of the Bomem MB-100 infrared spectrometer was controlled by the software package Spectra-Calc running on an IBM-386 type computer. Spectra typically were recorded at equal time intervals over a range of 1600−2300 cm^{-1}. Locally developed software was used to extract the absorbance at wavenumbers of interest for subsequent analysis on an IBM 486-type computer. The numerical integration program uses a fourth-order Runge−Kutta procedure. The fitting allows the delay time between mixing and the start of observation to be varied, and this was typically 200−300 s, as expected for transfer to the cell and temperature equilibration after handling.

Acknowledgment. We thank the Natural Sciences and Engineering Research Council of Canada for financial support for this work under the Cooperative Grants Program. We thank Dr. R. McDonald for the X-ray structure determination and Dr. G.-Y. Kie for preliminary synthetic work and for the synthesis and characterization of $Os(CO)_3(PMe_3)(\eta^2\text{-}C_2H_2)$ (**2**).

Supporting Information Available: Additional figures and Tables S1−S4, giving a summary of the X-ray analysis, atomic coordinates, anisotropic thermal parameters, and bond distances and angles. This material is available free of charge via the Internet at http://pubs.acs.org.

OM990007T

(19) Sheldrick, G. M. *Acta Crystallogr.* **1990**, *A46*, 467.
(20) Sheldrick, G. M. SHELXL-93: Program for Crystal Structure Determination; University of Göttingen, Göttingen, Germany, 1993.
(21) Walker, N.; Stuart, D. *Acta Crystallogr.* **1983**, *A39*, 158.
(22) Nudelman, N. S.; Doctorovich, F. *J. Chem. Soc., Perkin Trans.* **1994**, 1233 and references therein. Poë, A. J.; Sampson, C. N.; Smith, R. T.; Zheng, Y. *J. Am. Chem. Soc.* **1993**, *115*, 3174 and references therein. Field, L. R.; Wilhelm, E.; Battino, R. *J. Chem. Thermodyn.* **1974**, *6*, 237.